Climate control of a bulk storage room for foodstuffs

S. van Mourik, H. Zwart, Twente University,
K.J. Keesman*, Wageningen University, The Netherlands

Corresponding author: S. van Mourik
Department of Applied Mathematics
University of Twente, The Netherlands
Phone: +31 (53) 489 3473 , Fax: +31 (53) 489 3800
e-mail: s.vanmourik@ewi.utwente.nl
* Systems & Control Group
Wageningen University, The Netherlands
e-mail: Karel.Keesman@wur.nl

Abstract A storage room contains a bulk of agricultural products, such as potatoes, onions, fruits, etcetera. The products produce heat due to respiration, see for example [1, 2]. A ventilator blows cooled air around to keep the products at a steady temperature and prevent spoilage. The aim is to design a control law such that the product temperature is kept at a constant, desired level. The system contains nonlinear coupled partial differential equations (pde's). The assumptions that the input switches between discrete values, and that the system states have either very slow or very fast dynamics, simplify the equations. Transfer functions of the linear subsystems give us an idea of the time scales of the states, and with their approximations we can convert linear pde's into ordinary differential equations (ode's). The control problem for the simplified system consists of the determination of the switching moment, and is relatively easily solved.

1 The storage room

We consider a closed storage room with a bulk of products, Figure 1. The air temperature $T_a(x,t)$ is regulated by a ventilator that blows the air through the shaft and through the bulk. A cooling element, with variable temperature $T_c(t)$, is placed right below the ventilator. This means that if the ventilator blows harder, the air is cooled down more. The speed of the ventilator and the temperature of the cooling element are the control input. The aim is now to design a control law such that the product temperature, the controlled variable, is kept at a constant, desired level.

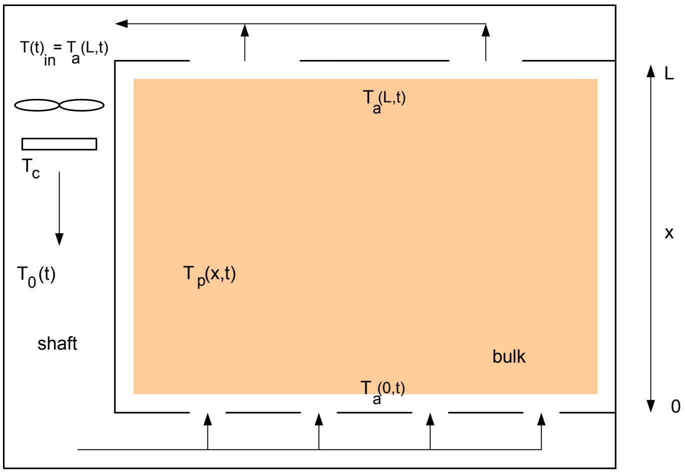

Figure 1: Bulk storage room

1.1 The model

The following assumptions are made:

- The walls are perfectly insulated;
- The air temperature in the shaft, $T_0(t)$, is well-mixed and therefore uniform over the length of the shaft;
- The air- and product temperature in the bulk, T_a and T_p, only vary with the height of the bulk, and so not with the width;
- Diffusion in the air is neglected since convection will dominate the heat transport;
- No moisture is incorporated in the model;
- The products are spherical;
- There is no heat exchange between products, but only between the products and the air.

These assumptions lead to the following energy balance. The energy inflow (J/s) of the air in the ventilator shaft is modelled in the basic way: $\rho c\Phi(\alpha T_c(t) + (1-\alpha)T_{in}(t))$, with ρ the air density, c the heat capacity, and Φ the volume flow of air through the shaft. The dimensionless constant α denotes the effectiveness of the cooling device; $\alpha = 1$ implies that the incoming air, $T_{in}(t)$, is totally cooled down (or heated up) to the temperature of the cooling element, $T_c(t)$, while $\alpha = 0$ implies that the incoming air is not cooled at all. We assume that α is independent of Φ. Because of the perfect insulation, we have that $T_{in}(t) = T_a(L,t)$. The energy outflow equals $-\rho c\Phi T_0(t)$. The dynamic energy balance for $T_0(t)$ therefore equals

$$\rho c V \frac{\partial T_0(t)}{\partial t} = -\rho c\Phi\alpha(T_a(L,t) - T_c(t)) + \rho c\Phi T_a(L,t) - \rho c\Phi T_0(t) \quad (J/s), \tag{1}$$

with V the volume of the shaft.
The energy balance for $T_a(x,t)$ is, with $x \in (0,L)$,

$$\rho c V_2 \frac{\partial T_a(x,t)}{\partial t} = -V_2\rho c v\frac{\partial T_a(x,t)}{\partial x} + h(v)A_p(T_p(R,x,t) - T_a(x,t)) \quad (J/s\ m^3), \tag{2}$$

with boundary condition

$$T_a(0,t) = T_0(t). \tag{3}$$

Here, V_2 is the air volume per bulk volume, A_p the product surface area per bulk volume, and $T_p(R,x,t)$ is the product surface temperature at x. The two r.h.s. terms in (2) denote the convection of heat and the heat exchange between product surface and air respectively. The parameter h depends on v via the implicit relation (see [1])

$$\mathrm{Nu} \quad = \quad (0.5\mathrm{Re}^{1/2} + 0.2\mathrm{Re}^{2/3})\mathrm{Pr}^{1/3} \quad \text{for} \quad 10 < \mathrm{Re} < 10^4, \tag{4}$$

with Nu, Re and Pr the Nusselt-, Reynolds- and Prandtl number, see the appendix.
The heat transport inside a product at height x is modelled by diffusion in a 3D sphere with radius R.

$$\rho_p c_p \frac{\partial T_p(r,x,t)}{\partial t} = \lambda\frac{1}{r^2}\frac{\partial}{\partial r}(r^2\frac{\partial T_p(r,x,t)}{\partial r}) + \rho_p a T_p(r,x,t) + \rho_p b \quad (J/m^3 s), \tag{5}$$

where ρ_p, c_p, and λ are the product density, heat capacity and conductivity, respectively. The last two terms in (5) denote the heat production, which is modelled according to [1]. The boundary conditions are

$$\begin{aligned} \frac{\partial T_p}{\partial r}(x,0,t) &= 0 \text{ by symmetry at the origin} \qquad (6)\\ \lambda\frac{\partial T_p}{\partial r}(x,R,t) &= h(v)(T_a(x,t) - T_p(R,x,t)) \text{ heat flux through the surface.} \end{aligned}$$

We impose the following additional assumptions

- $b \approx 0$, because typically $aT_p \gg b$. This simplifies the analysis in the next section;
- The product has no skin;
- $T_p(r, x, t)$ is regarded as a continuous medium in x. The heat flux between air and product surface at x is modelled as the flux between a sphere with a uniform air temperature $T_a(x, t)$ along its surface;

The last assumption can be justified by showing that the consequent maximal error in the transfer function from $\widehat{T}_p(R, x, s)$ to $\widehat{T}_a(x, s)$ is small.
The equations are nonlinear since v enters equation (1) by $\Phi = A_f v$, with A_f the surface of the bulk floor, and equation (2) via equation (4). The control objective is to regulate T_p, and the control variables are v and T_c.

1.2 Conclusions from the model

The equations are nonlinear and coupled. Because of their complex form, a control law cannot be obtained adequately by standard control design, such as e.g. optimal control. Fortunately, for constant $v(t)$, the equations are linear. Therefore, we can compute the transfer functions that connect the air- and product temperatures in the frequency domain. So we constrain $v(t)$ and $T_c(t)$ to only discrete values. The control law now consists of determining the optimal switching time instances and the choice of the size of the time interval in which v and/or T_c are switched.

2 System analysis

We want to take three system states, $T_p(R, L, t)$, $T_a(L, t)$ and $T_0(t)$. The transfer functions that connect these states in the frequency domain can tell us something about the timescales of their dynamics. Also, these transfer functions can be approximated by simple rational ones. First, the orders of the time constants of the uncoupled subsystems are determined. We emphasize that the analysis on the uncoupled subsystems only gives a global impression on the orders of the timescales. The interaction between the coupled states may change the time constants considerably. To be sure, we check the outcome on the full, coupled system. The physical parameters that are used, are for potatoes and are listed in Table 1.

2.1 Time constants of the product

The heat transfer between the air and the product surface is in the frequency domain

$$\widehat{T}_p(R, x, s) = G_p(s)\widehat{T}_a(x, s). \tag{7}$$

The transfer function $G_p(s)$ is a transcendental function and is approximated by a rational one in order to obtain its time constant. This is done with a Padé[0,1] approximation in $s = 0$ (see appendix)

$$G_p(s) \approx \frac{a_1}{a_2 + a_3 s}. \tag{8}$$

Transformation to the time domain gives

$$\frac{\partial T_p(R, x, t)}{\partial t} = -\frac{a_2}{a_3} T_p(R, x, t) + \frac{a_1}{a_3} T_a(x, t), \tag{9}$$

with

$$\begin{aligned} a_1 &= Bi \\ a_2 &= 2M_3\cot(M_3) - 2 + Bi \\ a_3 &= \frac{R^2}{M_1}\cot^2(M_3) + \frac{R^2}{M_1} - \frac{M_3}{M_2}\cot(M_3). \\ M_1 &= \frac{\lambda}{\rho_p c_p};\ \text{diffusion coefficient}\ \ (m^2/s) \\ M_2 &= \frac{a}{c_p};\ \text{reaction constant}\ \ (1/s) \\ M_3 &= \sqrt{M_2/M_1}R;\ \frac{\text{chemical reaction rate}}{\text{diffusive heat transfer rate}}. \end{aligned} \tag{10}$$

The dimensionless parameter M_3 is analogous to the Thiele modulus

$$Th = \frac{\text{chemical reaction rate}}{\text{diffusive mass transfer rate}}. \tag{11}$$

Bi is the Biot number (see appendix) and $Bi \approx 2$. The time constant of $G_p(s)$ is a_3/a_2 and is $\mathcal{O}(10^3)$. The time constant for heat transfer from bulk air to *within* the sphere is even higher, because $Bi \gg 0.1$. This means that the heat transport from the product surface to the core takes a long time (see [3], chapter 4.2). We conclude that T_p has slow dynamics.

2.2 Time constants of the air temperatures

The time constants of T_0 are obtained from the transfer functions that correspond to equation (1)

$$\begin{aligned} \widehat{T}_0(s) &= G_3(s)\widehat{T}_a(L,s) + G_4(s)\widehat{T}_c(s) \\ &= \frac{1-\alpha}{1+\frac{V}{\Phi}s}\widehat{T}_a(L,s) + \frac{\alpha}{1+\frac{V}{\Phi}s}\widehat{T}_c(s). \end{aligned} \tag{12}$$

The time constants are both equal to $\frac{V}{\Phi}$. Therefore, the time constant of this subsystem equals $\frac{V}{\Phi}$.

The transfer function corresponding to equation (2) is

$$\widehat{T}_a(x,s) = \int_0^x \frac{M_4}{v}\exp\left(\frac{s+M_4}{v}z\right)\widehat{T}_p(R,z,s)dz\exp\left(-\frac{s+M_4}{v}x\right) + \widehat{T}_0(s)\exp\left(-\frac{s+M_4}{v}x\right), \tag{13}$$

with $M_4 = \frac{hA_p}{V_2\rho c}$. This expression is not of the form

$$\widehat{T}_a(x,s) = G_1(s,x)\widehat{T}_0(s) + G_2(s,x)\widehat{T}_p(R,x,s), \tag{14}$$

and therefore we make an approximation by taking $T_p(R,x,t)$ uniform in x. The corresponding transfer functions are now

$$\begin{aligned} G_1(s,x) &= \exp\left(-\frac{s+M_4}{v}x\right) \\ G_2(s,x) &= \frac{M_4(1-\exp\left(-\frac{s+M_4}{v}x\right))}{s+M_4}. \end{aligned} \tag{15}$$

They are not rational since they contain a time delay x/v. Hence, we cannot see their time constants directly. The Padé[0,1] approximations in $s=0$ are given by

$$\begin{aligned} G_1(s,x) &\approx \frac{1}{\exp\left(\frac{M_4x}{v}\right) + \frac{x}{v}\exp\left(\frac{M_4x}{v}\right)s} \\ G_2(s,x) &\approx \frac{2(\cosh(\frac{M_4x}{v})-1)}{\exp\left(\frac{M_4x}{v}\right) - 1 + \frac{1}{M_4}(\exp\left(\frac{M_4x}{v}\right) - 1 - \frac{M_4x}{v})s}, \end{aligned} \tag{16}$$

with $M_4 = \frac{hA_p}{V_2\rho c}$ the reaction constant of the product heat production $(1/s)$. The approximations have time constants

$$\begin{array}{rl} \dfrac{x}{v} & (\text{ at most } \mathcal{O}(10^0) \text{ in } x = L) \\ \dfrac{\frac{1}{M_4}\left(\exp\left(\frac{M_4x}{v}\right) - 1 - \frac{M_4x}{v}\right)}{\exp\left(\frac{M_4x}{v}\right) - 1} & (\text{ at most } \mathcal{O}(10^0) \text{ in } x = L). \end{array} \tag{17}$$

We have that the dimensionless number

$$M_5 = \frac{M_4L}{v}; \quad \frac{\text{chemical reaction rate}}{\text{convective heat transfer rate}} \tag{18}$$

is analogous to the Damköhler I number

$$\text{Da I} = \frac{\text{chemical reaction rate}}{\text{convective mass transfer rate}}. \tag{19}$$

2.3 Coupled dynamics

The interaction between the states complicates the analysis. However, we try to derive some global properties of the coupled system in an ad-hoc manner. The starting point is that $T_a(L,t)$ is constant, and that $T_c(t)$ switches. Then $T_0(t)$ quickly settles to a new value because of the small time constant of $G_4(s)$ in (12). We split up (14) into

$$\begin{aligned} \widehat{T}_a(L,s) &= G_1(s,L)\widehat{T}_0(s) + G_2(L,s)\widehat{T}_p(R,L,s) \\ &= \widehat{T}_{a1}(L,s) + \widehat{T}_{a2}(L,s). \end{aligned} \tag{20}$$

$T_{a1}(L,t)$ will settle quickly because of the small time constant of $G_1(s,L)$. $T_{a2}(L,t)$ adapts itself quickly to $T_p(R,L,t)$, but since $T_p(R,L,t)$ moves slowly (because of the large time constant of $G_p(s)$), $T_{a2}(L,t)$ will also move slowly. $T_a(L,t)$ is dominated by $T_{a2}(L,t)$ since $|G_2(s,L)| \gg |G_1(s,L)|\ \forall s \in i\mathbb{R}$. Hence, after a switch, the fast change of $T_a(L,t)$ will be small. This justifies the starting-point that $T_a(L,t)$ is constant.

If v is switched, then we observe the following. The order of the time constants remain the same if v_1 and v_2 are of the same order. If v increases, then the static gain $|G_1(0,L)|$ in (15) and (16) increases, whereas $|G_2(0,L)|$ decreases. So $T_a(L,t)$ will be dominated less by $T_p(R,L,t)$ than before, and more by $T_0(t)$. As a result, $T_a(L,t)$ will cool down. $T_a(L,t)$ will settle quickly because $G_1(s,L)$ and $G_2(s,L)$ have small time constants.

2.4 Full system in state space form

We looked at the time constants of the uncoupled subsystems, with the assumption that T_p is uniform in x. The analysis of the time constants is checked numerically on the (coupled) full system. The full system consists of equations (1), (2), and (9). We look at the full system dynamics by means of eigenvalue analysis and time simulation. The equations are discretised as follows. The term $v\frac{\partial T_a}{\partial x}$ in (2) is upwind discretised like $v\frac{T_{a,n}-T_{a,n-1}}{\delta x}$, where the second subscript denotes the discrete space. The spatially discretised total system has the form

$$\frac{\partial T}{\partial t} = A(v)T + B(v)T_c, \tag{21}$$

with $T = [T_{a,1}..T_{a,n}\ T_0\ T_{p,1}..T_{p,n}]^T$. Subscript 1 denotes $x = 0$, and n denotes $x = L$. This differential equation is simulated in Simulink with the ode45 Dormand-Prince algorithm. The physical parameters of the chosen configuration are listed in Table 1. For these constants, $Re = 1.9\ 10^3$, so we may use equation (4). The inverse eigenvalues of $A(v)$ of the full (coupled) system are compared to the time constants of the uncoupled subsystems. Table 2 shows that for $n = 2$ the orders of the time constants of the total system match those of the uncoupled systems. For larger n, the

α	0.5	T_{ini}	288
R	0.0325	V	10
L	2	v	0.5
λ	0.55	ρ_p	1014
a	$1.9\ 10^{-3}$	A_p	49
V_2	0.61	c_p	$3.6\ 10^3$
T_c	276	A_f	5

Table 1: Physical parameters of a bulk with potatoes. The data specific for potato were taken from [1, 2].

subsystems	full system
2.26e3	8.43e3
-	3.00e4
4.00	4.08
-	0.73 + 0.04i
0.85	0.73 + 0.04i

Table 2: Inverse eigenvalues of the full system and time constants of the three uncoupled subsystems.

resemblance becomes better, but a difference will remain, because we compare dynamics of states $T_a(L,t), T_0(t)$, and $T_p(R,t)$ to the spatially distributed state vector $[T_{a,1}..T_{a,n}\ T_0\ T_{p,1}..T_{p,n}]^T$.

The time constants of the full system contain an imaginary part. This is probably due to the high condition number of $A(v)$ of $\mathcal{O}(10^7)$. Time simulations therefore show oscillations, but when the state vectors of T_p, T_0 and T_a are simulated in parallel, the oscillations do not show.

The (real parts of the) eigenvectors of the full system are shown in Table 3. The two left eigenvectors correspond to the small eigenvalues and thus to the large timescales. These are the only ones that have substantial components in the directions $T_{p,1}(t)$ and $T_{p,2}(t)$. So T_p has only slow dynamics. This is in agreement with the analysis of the uncoupled subsystems from the previous section. The two 'slow' eigenvectors also have substantial components in the other directions, so the 'fast' states T_0 and T_a also have slow dynamics. We conclude that the fast state dynamics are coupled to the slow ones; they settle quickly and slowly move along with the slow states. This also in agreement with the previous section. From the inverse eigenvalues we see that the time constant of the slow states are $\mathcal{O}(10^3)$, and the time constants of the fast states are $\mathcal{O}(10^0)$. The switching interval should therefore be chosen in the order of $10^1 - 10^2$.

2.5 Time simulation

The initial product- and air temperatures are 288 K, and we let T_c switch between 276 K and 248 K every five minutes. Total simulation time is 20 hours. Figure 2 shows $T_{p,n}(t)$ for $n = 2, 10$ and 20. For reasonable accuracy we need $n = 10$, which comes to 21 states in total. Figure 3 shows $T_{p,n}(t)$ and $T_{a,n}(t)$ on an interval of 10 minutes at the moment of steepest descent of $T_{p,n}(t)$. $T_{a,n}(t)$ settles quickly after a switch, whereafter it moves slowly along with T_p. After a switch, $T_0(t)$ and $T_c(t)$ (both not shown here) change considerably, whereas $T_a(L,t)$ changes only a little.

$T_{a,1}$	0.35	-0.31	0.22	-0.01	-0.01
$T_{a,2}$	0.56	0.49	0.05	0.95	0.95
T_0	0.22	0.20	0.97	-0.09	-0.09
$T_{p,1}$	0.38	-0.42	-0.04e-2	0.08e-4	0.08e-4
$T_{p,2}$	0.61	0.67	-0.01e-2	-0.03e-2	-0.03e-2

Table 3: State space vector (most left) and the eigenvectors of the full system for $n = 2$.

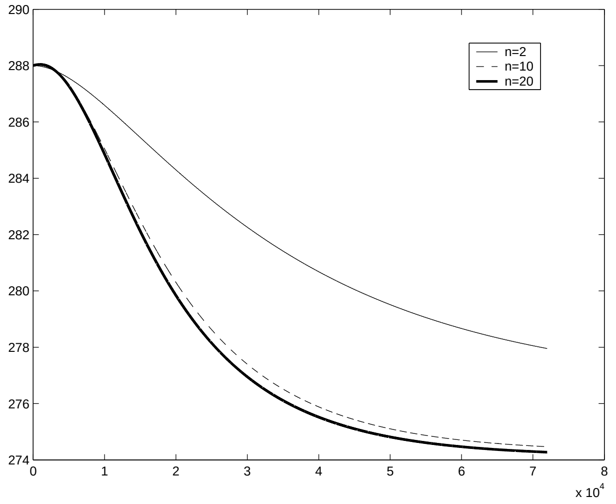

Figure 2: Simulation of the cooling of $T_{p,n}(t)$ for $n = 2, 10$ and 20.

Hence, the influence of $T_0(t)$ on $T_a(L, t)$ is very small, in agreement with the analysis from the previous section. Further, the states are all more or less constant during one switching interval.

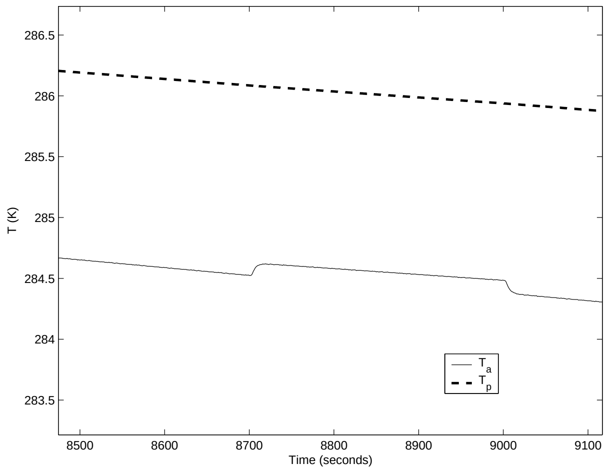

Figure 3: The steepest descent of $T_{p,n}(t)$ and $T_{a,n}(t)$ during the cooling process.

3 Switching time

Because T_p has its highest values at the top of the bulk, we want to control $T_p(R, L, t)$. Suppose $T_p(R, L, t)$ is at its ideal value $T_{p,opt}(R, L)$. The question is now when to switch T_c or v (or both) such that $T_p(R, L, t)$ maintains its ideal value. In the previous section it was shown that on a timescale of 5 minutes, $T_p(R, L, t)$ and $T_a(L, t)$ are approximately constant due to the fast settling of $T_a(L, t)$ and the slow dynamics of $T_p(R, L, t)$. $T_a(L)$ can therefore be computed from the static equations (1) and (2). This gives

$$\begin{aligned} T_0 &= (1-\alpha)T_a(L) + \alpha T_c \qquad (22) \\ T_a(L) &= \left[\int_0^L \frac{M_4}{v} \exp\left(M_5\right) T_p(R,x)dx + T_0\right] \exp\left(-M_5\right) \\ \Rightarrow T_a(L) &= \left(1-(1-\alpha)\exp\left(-M_5\right)\right)^{-1} \left[\int_0^L \frac{M_4}{v} \exp\left(M_5\right) T_p(x)dx + \alpha T_c\right] \exp\left(-M_5\right). \end{aligned}$$

Note that in order to solve for (22), one needs to know the spatial distribution of $T_p(R,x)$. The optimal air temperature is computed from the static equation (9), which gives

$$T_{a,opt}(L) = \frac{a_2}{a_3} T_{p,opt}(L). \qquad (23)$$

The switching time, such that the average $T_a(L)$ is optimal,

$$\int_0^\tau T_{a,1}(L)dt + \int_\tau^{\tau_f} T_{a,2}(L)dt = \tau_f T_{a,opt}(L), \qquad (24)$$

where subscripts 1 and 2 denote the inputs $v_1, T_{c,1}$ and $v_2, T_{c,2}$, has the solution

$$\begin{aligned} \tau &= \frac{\tau_f(T_{a,opt} - T_{a,2}(L))}{T_{a,1}(L) - T_{a,2}(L)} \quad \text{if} \quad (v,T_c) = (v_1, T_{c,1}) \quad \text{at} \quad t=0 \qquad (25) \\ \tau &= \frac{\tau_f(T_{a,opt} - T_{a,1}(L))}{T_{a,2}(L) - T_{a,1}(L)} \quad \text{if} \quad (v,T_c) = (v_2, T_{c,2}) \quad \text{at} \quad t=0. \end{aligned}$$

4 Conclusion

We have modelled the storage room by one ordinary differential equation and two partial differential equations. The resulting system equations are simplified using three techniques; timescale separation, discrete switching input, and Padé approximation of a transfer function. The transfer functions of the simplified system give a good indication of the timescales, and also show how the fast dynamics are coupled to the slow dynamics. These properties are checked by analysis of the discretized full system. For the simplified system, the switching time τ is completely parametrized. This gives an algorithm for keeping $T_p(R,L,t)$ at a constant value. The methodology used here seems extendable to more complex models which incorporate, for example, moisture transport and heat loss through the walls.

The next step will be the construction of a controller to steer $T_p(R,L,t)$. The input will be $T_a(L,t)$. The discrete time steps, in which the controller prescribes the optimal input, are then equal to τ_f. By continuous adjustment of τ, the average $T_a(L)$ over the switching interval is set to its prescribed value.

5 Acknowledgement

This work was supported by the Technology foundation STW under project number WWI.6345.

References

[1] Xu, Y., Burfoot, D., Simulating the bulk storage of foodstuffs. Journal of food engineering 39, 1999, 23-29.

[2] Keesman, K.J., Peters, D., Lukasse, L.J.S., Optimal climate control of a storage facility using local weather forecasts. Control Engineering Practice 11, 2003, 505-516.

[3] White, F.M., Heat and mass transfer. Addison-Wesley, 1988.

Appendix

A.1 Construction of a transfer function

A transfer function of a linear pde in the variables x and t is constructed by substituting $\partial/\partial t = s$ and solving the ode for the variable x. The solution can be written as $\widehat{y}(s,x) = G(s,x)\widehat{u}(s,x)$, with $\widehat{y}(s,x)$, $\widehat{u}(s,x)$ and $G(s,x)$ the output, input and the transfer function, respectively.
If $G(s,x)$ is of the form

$$\frac{a_0 s^0 + .. + a_n s^n}{b_0 s^0 + .. + b_m s^m}, \tag{26}$$

i.e. rational, then the transfer function for a fixed x can be transformed back into a linear ode in t, and its time constant can be determined. If not, the nonrational transfer function can be approximated by a rational one, for example by a Padé approximation.

A.2 Padé approximation

A Padé[0,1] approximation in $s = 0$ has the form

$$\tilde{G}(s,x) = \frac{1}{\frac{a_2}{a_1}(x) + \frac{a_3}{a_1}(x)s}, \tag{27}$$

and the coefficients are determined by setting

$$\begin{aligned} G(0,x) &= \tilde{G}(0,x) \\ \frac{\partial G}{\partial s}(0,x) &= \frac{\partial \tilde{G}}{\partial s}(0,x). \end{aligned}$$

A clever choice of n and m in a Padé$[n,m]$ approximation is made by observation of the Bode plot of the original transfer function.

A.3 Notation

α	cooling effectiveness	T_p	produce temperature (K)
α_{th}	thermal diffusivity of air (1.87e-5 m^2/s)	T_a	air temperature in the bulk (K)
λ	conduction of product $(W/m\ K)$	T_c	cooling element temperature (K)
λ_{air}	conduction of air (2.43e-2 $W/m\ K$)	τ_f	length of switching interval (s)
ρ_p	produce density (kg/m^3)	T_{ini}	initial temperature (K)
ρ	air density (1.27 kg/m^3)	V	volume of shaft (m^3)
τ	switching time (s)	V_2	porosity (m^3/m^3)
ν	kinematic viscosity of air (1.3465e-5 m^2/s)	c_p	heat capacity of produce $(J/kg\ K)$
a	product heat production $(J/kg\ s\ K)$	c	heat capacity of air (1000 $J/kg\ K$)
b	product heat production $(J/kg\ s)$	h	heat transfer coefficient (W/m^2K)
R	product radius (m)	v	air velocity through bulk (m/s)
A_p	produce surface per bulk volume (m^2/m^3)	Φ	air flow through shaft (m^3/s)
A_f	floor area of the bulk (m^2)	M_1	$\frac{\lambda}{\rho_p c_p}$
L	bulk height (m)	M_2	$\frac{a}{c_p}$
L_2	$R * por(1 - por)$, char. length (m)	M_3	$\sqrt{M_2/M_1}R$
Bi	Biot number $\frac{2hR}{\lambda}$	M_4	$\frac{hA_p}{V_2 \rho c}$
Re	Reynolds number $\frac{vL_2}{\nu}$, see [1]	M_5	$\frac{M_4 L}{v}$
Nu	Nusselt number $\frac{2hR}{\lambda_{air}}$	Pr	Prandtl number $\frac{\nu}{\alpha_{th}}$